Vortices in a wedge made of a type-I superconductor

2015 New J. Phys. 17 063032

(http://iopscience.iop.org/1367-2630/17/6/063032)

New Journal of Physics
The open access journal at the forefront of physics

Deutsche Physikalische Gesellschaft DPG
IOP Institute of Physics

Published in partnership with: Deutsche Physikalische Gesellschaft and the Institute of Physics

OPEN ACCESS

RECEIVED
2 April 2015

REVISED
27 May 2015

ACCEPTED FOR PUBLICATION
2 June 2015

PUBLISHED
25 June 2015

PAPER

Vortices in a wedge made of a type-I superconductor

V N Gladilin[1,2,3], J Ge[1], J Gutierrez[1], M Timmermans[1], J Van de Vondel[1], J Tempere[2], J T Devreese[2] and V V Moshchalkov[1]

[1] INPAC—Institute for Nanoscale Physics and Chemistry, KU Leuven, Celestijnenlaan 200D, B-3001 Leuven, Belgium
[2] TQC—Theory of Quantum and Complex Systems, Universiteit Antwerpen, Universiteitsplein 1, B-2610 Antwerpen, Belgium
[3] Author to whom any correspondance should be addressed.

E-mail: vladimir.gladilin@uantwerpen.be

Keywords: superconductor, vortex, Ginzburg–Landau theory

Supplementary material for this article is available online

Abstract

Using the time-dependent Ginzburg–Landau approach, we analyze vortex states and vortex dynamics in type-I superconductor films with a thickness gradient in one direction. In the thinnest part of the structures under consideration, the equilibrium states manifest the typical type-II vortex patterns with only singly-quantized vortices. At the same time, in the regions with larger thickness the singly-quantized and giant vortices coexist, in a qualitative agreement with our scanning Hall probe microscopy measurements on relatively thick Pb films. In the presence of an external current applied perpendicularly to the thickness gradient direction, the singly-quantized vortices, which enter the wedge through its thinnest edge, merge into giant vortices when propagating to the thicker parts of the structure. Remarkably, the results of our simulations imply that at moderate external current densities a regime is possible where the winding number of giant vortices, formed as a result of vortex coalescence, takes preferentially (or even exclusively) the values given by positive integer powers of two.

1. Introduction

Single-band superconductors are commonly subdivided into two types with qualitatively different vortex behaviour depending on the value of the Ginzburg–Landau parameter $\kappa = \lambda/\xi$, where ξ is the coherence length and λ is the penetration depth of the superconducting material. In type-II superconductors, with $\kappa > 1/\sqrt{2}$, purely repulsive vortex–vortex interaction leads to the formation of the famous Abrikosov lattice of singly-quantized vortices at magnetic fields above the first critical field [1]. In type-I superconductor slabs, characterized by $\kappa < 1/\sqrt{2}$, the vortex–vortex interaction, still long-range repulsive, becomes attractive at short intervortex distances. As a result, in the intermediate state of a type-I superconductor, vortices merge into macroscopic multiquanta flux domains of different shape, for instance bubble-like. The size and magnetic flux of those bubbles are shown to increase with increasing the superconductor slab thickness [2]. As concerns singly-quantized vortices in a type-I superconductor, the possibility of their coexistence with multiquanta fluxoids (giant vortices) was theoretically predicted for mesoscopic samples [3]. More recently, it was experimentally demonstrated that singly-quantized vortices can be stabilized in the intermediate state of a relatively thick macroscopic type-I superconductor film [4].

The vortex–vortex interactions in type-I superconductor films are known to strongly depend on the film thickness d [5–7]: at $d < \lambda$ these interactions are determined by an effective penetration depth $\Lambda \sim \lambda^2/d$ rather than by the bulk value λ. Therefore, in sufficiently thin films of type-I superconductors (and also thin wires—see e.g. [8]), where the effective Ginzburg–Landau parameter Λ/ξ exceeds $1/\sqrt{2}$, vortex behaviour is type-II-like, so that only singly-quantized vortices are stable there. In the present paper, we consider a type-I superconductor with a uniform thickness gradient (superconducting wedge). Our goal is to analyze the coexistence of types-I and II vortex behaviours within a single sample as well as transformations of vortices moving from the effectively

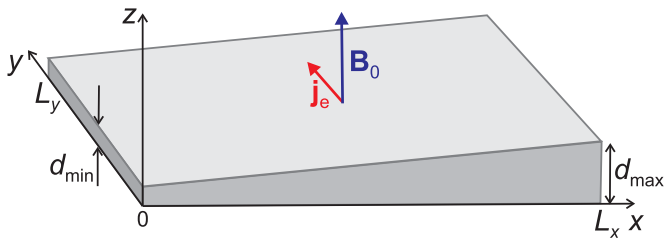

Figure 1. Structure under consideration. The thickness of a type-I superconductor film with lateral sizes $L_x \times L_y$ linearly increases in the x direction from d_{min} at $x = 0$ to d_{max} at $x = L_x$. The applied magnetic field B_0 is parallel to the z axis. The external current is applied in the y direction.

type-II region to the type-I region of the wedge. The vortex states and vortex dynamics are numerically calculated using the time-dependent Ginzburg–Landau (TDGL) formalism for superconducting films with variable thickness [12].

The remaining part of the paper is organized as follows. In section 2 we describe the system under consideration and the TDGL formalism, used to calculate static and dynamic distributions of the order parameter as well as the corresponding magnetic and electric fields. The simulation results are given in section 3 where we first discuss the equilibrium vortex patterns in a superconductor wedge and then focus on the dynamics and transformations of vortices, which move in the direction of the thickness gradient. The main conclusions are drawn in section 4.

2. Theoretical model

We consider a type-I superconductor with the shape shown in figure 1. The lateral sizes of the thin superconducting 'wedge', L_x and L_y, are much larger than the thickness $d(x)$, which varies linearly from d_{min} at $x = 0$ to d_{max} at $x = L_x$. An external homogeneous magnetic field B_0 is applied along the z axis. When studying the vortex dynamics in the wedge, an external current is applied in the y direction. In order to ensure the coexistence of both types-I and II vortex behaviours within the wedge, its thickness has to vary from a small fraction of the bulk penetration depth λ to a value significantly larger than λ. For the structures with lateral sizes $\lesssim 400\lambda$, which are analysed below, this requirement leads to a relatively large thickness gradient $|\nabla d| > 0.01$. As a result, the so-called type-II/1 phase (see e.g. [13–15] and references therein), which could be expected when the effective Ginzburg–Landau Λ/ξ parameter lies in the close vicinity of $1/\sqrt{2}$, appears to be irrelevant: for the wedges under consideration, the width of the corresponding region is comparable to or even smaller than the vortex size.

Vortex states and vortex dynamics are described using the TDGL formalism. Although the applicability of the Ginzburg–Landau theory can be rigorously substantiated only when the temperature of a superconductor is close to the critical temperature T_c [9], in practice this theory is known to provide correct qualitative or even semi-quantitative predictions for a much wider temperature range. This concerns, in particular, an adequate description of stable vortex states (see e.g. [10] and references therein) and vortex dynamics (see e.g. [11]) in relatively small samples with sizes comparable to those in our present calculations.

Assuming that the thickness d_{max} is smaller than or comparable to the coherence length ξ of the superconductor, an effectively two-dimensional TDGL equation for the order parameter ψ, normalized to 1 and averaged over $d(x)$, in a superconductor with varying thickness can be written as [12]

$$\left(\frac{\partial}{\partial t} + i\varphi\right)\psi = \frac{1}{d}(\nabla_2 - i\mathbf{A})d(\nabla_2 - i\mathbf{A})\psi + 2\psi(1 - |\psi|^2). \quad (1)$$

Here, φ and $\mathbf{A}$ are the scalar and vector potentials, respectively, averaged over the superconductor thickness $d(x)$, and $\nabla_2 = \mathbf{e}_x\partial/\partial x + \mathbf{e}_y\partial/\partial y$. All the relevant quantities are made dimensionless by expressing lengths in units of $\sqrt{2}\,\xi$, time in units of $\pi\hbar/[4k_B(T_c - T)] \approx 11.6\tau_{GL}$, magnetic field in units of $\Phi_0/(4\pi\xi^2) = \mu_0 H_{c2}/2$, current density in units of $\Phi_0/[2\sqrt{2}\,\pi\mu_0\lambda^2\xi] = 3\sqrt{3}/(2\sqrt{2})j_c$, and scalar potential in units of $2k_B(T_c - T)/(\pi e)$. Here, $\Phi_0 = \pi\hbar/e$ is the magnetic flux quantum, μ_0 is the vacuum permeability, λ is the penetration depth at a given temperature T, τ_{GL} is the Ginzburg–Landau time, H_{c2} is the second critical field, and j_c is the critical (depairing) current density of a thin wire or film [16].

The distribution of the scalar potential φ is determined from the condition $\nabla \cdot \mathbf{j} = 0$, which reflects the continuity of currents in the superconductor. The total current density $\mathbf{j}$ is given by the sum of the normal and superconducting components:

$$\mathbf{j} = \mathbf{j}_n + \mathbf{j}_s, \tag{2}$$

$$\mathbf{j}_n = -\frac{\sigma}{2}\left(\nabla\varphi + \frac{\partial \mathbf{A}}{\partial t}\right), \tag{3}$$

$$\mathbf{j}_s = \mathrm{Im}\left(\psi^* \nabla\psi\right) - \mathbf{A}\,|\psi|^2, \tag{4}$$

where σ is the normal-state conductivity, which is taken as $\sigma = 1/12$ in our units [17]. For a thin superconductor with varying thickness the aforementioned condition of current continuity can be expressed [12] in a 2D form:

$$\frac{\sigma}{2}\nabla_2(d\,\nabla_2\varphi) = \nabla_2\left(\mathbf{j}_s d\right). \tag{5}$$

The averaged vector potential $\mathbf{A}$ that enters in equation (1) can be represented as

$$\mathbf{A} = \mathbf{A}_e + \mathbf{A}_s. \tag{6}$$

Here the contribution $\mathbf{A}_e = B_0(-\mathbf{e}_x y/2 + \mathbf{e}_y x/2)$ corresponds to the externally applied magnetic field $\mathbf{B}_0$, while $\mathbf{A}_s$ describes the averaged magnetic field, which is induced in the superconductor by the currents given by equations (2)–(4). For a thin superconducting layer with an x-dependent thickness, the latter contribution takes the form

$$\mathbf{A}_s(x, y, t) = \frac{1}{2\pi\kappa^2}\int_0^{L_x} \mathrm{d}x' d(x') \int_0^{L_y} \mathrm{d}y' K(x, x', |y - y'|)\mathbf{j}(x', y', t), \tag{7}$$

where $\kappa = \lambda/\xi$ is the Ginzburg–Landau parameter and the time-independent kernel

$$K(x, x', |y - y'|) = f(x, x', |y - y'|) + f(x', x, |y - y'|) \tag{8}$$

is expressed through the function

$$f(x, x', Y) = \frac{1}{d(x)}\left\{\ln\left[\frac{R\left(d(x'), |x - x'|, |y - y'|\right)}{R\left(d(x') - d(x), |x - x'|, Y\right)}\right]\right.$$

$$+ \frac{1}{2d(x')}\left[R\left(d(x') - d(x), |x - x'|, Y\right) + R\left(0, |x - x'|, Y\right)\right.$$

$$\left.\left. - R\left(d(x'), |x - x'|, Y\right) - R\left(-d(x), |x - x'|, Y\right)\right]\right\} \tag{9}$$

with

$$R(D, X, Y) = D + \sqrt{D^2 + X^2 + Y^2}. \tag{10}$$

Equation (1) with scalar and vector potentials defined by equations (5)–(7) are solved numerically using the approach described in [18–20]. The superconductor-insulator boundary conditions

$$\left(\frac{\partial}{\partial x} - \mathrm{i}A_x\right)\psi\Big|_{x=0,L_x} = 0, \quad j_{nx}\Big|_{x=0,L_x} = 0, \tag{11}$$

which assure zero values for both the superconducting and normal components of the current across the boundary, are assumed in the x-direction. Analogous boundary conditions are imposed in the y direction when simulating equilibrium vortex states. When studying vortex dynamics, at $y = 0$ and $y = L_y$ we take the normal metal-superconducor boundary conditions for the order parameter and the scalar potential

$$\psi|_{y=0,L_y} = 0, \qquad \frac{\partial\varphi}{\partial y}\Big|_{y=0,L_y} = -2j_e/\sigma, \tag{12}$$

where j_e is the average transport current density in the superconductor.

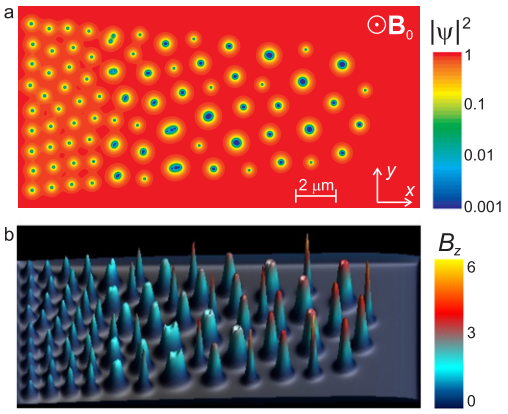

Figure 2. Calculated equilibrium distributions of the order parameter (a) and of the z component of the magnetic field averaged over the thickness of the superconductor thickness (b) for a wedge with $\xi = 250$ nm, $\lambda = 50$ nm, L_x=10 μm, L_y=20 μm, $d_{\min} = 20$ nm, and $d_{\max} = 200$ nm at $B_0 = 0.8$ in the absence of any applied currents. While in the thinnest part (at the left-hand side) of the wedge only single-quantum vortices appear, in the thicker part they coexist with giant vortices and vortex clusters.

3. Results and discussion

3.1. Equilibrium vortex states

When calculating the equilibrium vortex patterns, we start with a random distribution of the order parameter with $|\psi| \ll 1$ and alow the solution of equation (1) together with equations (5)–(7) to evolve towards a stable (metastable) state in the presence of a constant applied magnetic field B_0. A typical example of the resulting equilibrium distributions of the order parameter and the z component of the magnetic field in a type-I superconductor wedge is illustrated by figure 2. The shown plots correspond to a superconductor with $\xi = 250$ nm and $\lambda = 50$ nm. The thickness changes from $d_{\min} = 20$ nm at the lhs edge to $d_{\max} = 200$ nm at the rhs edge. In the thinnest part of the wedge, only vortices with the winding number (vorticity) $L = 1$ appear, reflecting an effectively type-II behaviour of the superconducting condensate in this region. At larger thicknesses of the superconductor, formation of giant vortices with $L \geqslant 2$, typical for the intermediate state of type-I superconductor films, becomes energetically favourable. From figure 2 one can also see that with increasing x (i.e. with increasing the superconductor thickness) the density of vortices gradually decreases and they are repelled farther from the edges of the superconductor.

Since the vortex-core size increases with L, for giant vortices it significantly exceeds the thickness of the superconductor under consideration (see figure 2(a)). For this reason, a giant vortex here can be seen as a flat 'current ring' rather than a long 'current tube' in relatively thick superconductor samples. The z component of the magnetic field, induced by such a current ring, has a circularly symmetric 'volcano-like' distribution (see figure 2(b)) instead of a bell-shaped magnetic field distribution, which corresponds to vortex tubes with radii much smaller than their length. With decreasing superconductor thickness, the giant vortices become less stable. As a result, in the left half of the superconductor sample the giant vortices are transformed into densely packed vortex clusters (figure 2(a)), which produce asymmetric 'volcanoes' in the magnetic field distribution shown in figure 2(b).

As follows from figure 2, due to the long-range vortex–vortex repulsion, some of singly-quantized vortices ($L = 1$) can remain stable even when they are nucleated in the thickest part of the sample, where the vortex behaviour corresponds to a type-I superconductor. This result is in line with the recent experimental observations [4] on a Pb film. In figure 3(a) we show a scanning Hall probe microscopy (SHPM) image taken on the same sample that was studied in [4]. Due to a relatively large thickness of the film (5 μm), the magnetic field distribution measured in the vicinity of the film surface can be adequately approximated by the monopole model [21, 22], which allows, in particular, to unambiguously quantify the winding number L for observed vortices(see e.g. [4, 23]). Thus, by fitting the field profiles of the vortices, shown in figure 3(a), with the monopole model (solid lines in figure 3(b)), we can see that giant vortices II and III coexist there with a singly quantized vortex labelled by I.

3.2. Vortex dynamics

When simulating the vortex dynamics in a superconductor wedge in the presence of a dc transport current, we assume that the current is applied in the positive y direction. The Lorentz force, caused by this current and the applied field, tends to move vortices in the positive x direction, i.e. from the thinner part of the superconductor

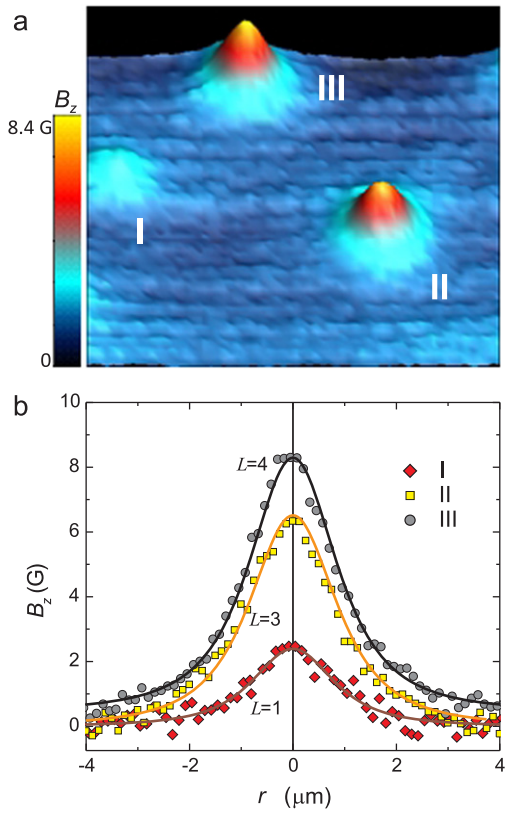

Figure 3. (a) $16 \times 16\,\mu m^2$ scanning Hall probe microscopy image taken at the temperature 6.5 K on a Pb film with thickness 5 μm after field cooling at B_0=1.2 G. (b) Field profiles along the cross-section for vortices labelled as I, II and III in panel (a). Fitting with the monopole model (solid lines) reveals the vorticity $L = 1$, 3 and 4 for vortices I, II and III, respectively.

to its thicker part. If the external current densities j_e are high enough, vortices can leave the superconductor through its rhs edge, while new vortices enter the wedge through the lhs edge. We focus on the stationary regime at those current densities. Figure 4 provides an example of the time evolution of the magnetic field pattern induced by the superconductor wedge in this regime. Vortices, which enter the wedge through its lhs edge, where the superconductor thickness is minimal, are singly quantized ($L = 1$). When propagating to the thicker part of the superconductor, vortices merge with each other, forming giant vortices with gradually increasing winding number L. As a result of this vortex coalescence process, individual vortices with $L = 1$ cannot reach the thicker (rhs) half of the of wedge and only giant vortices are present there—in contrast to the equilibrium vortex patterns in the absence of the transport current, which are described in the previous subsection. Singly-quantized vortices reappear only near the rhs edge of the wedge due to the fact that a giant vortex does not leave the superconductor at once: instead, singly-quantized vortices are split from a giant vortex and removed one by one, so that the vorticity of the remaining object step by step decreases down to 1.

At relatively low applied current densities j_e the vortex merger processes can result in a regime where the pattern of moving vortices has the form of bands of definite vorticity, which increases with increasing the local thickness of the superconductor. As an example, in figure 5 we show few snapshots of the order parameter distribution for a wedge with the thickness increasing from $d_{min} = 20$ nm to $d_{max} = 200$ nm in the x direction at $j_e = 0.05$ (see supporting information for the corresponding animations). As follows from figure 5, while in the vicinity of the lhs superconductor edge only vortices with $L = 1$ are present, the middle part of the superconductor contains only vortices with $L = 2$, which merge into vortices with $L = 4$ in the rhs part of the wedge (as discussed above, the latter step by step loose their vorticity when approaching the rhs edge closely). Remarkably, no vortices with $L = 3$ appear as a result of vortex coalescence. The reason is that only vortices with $L = 2$ reach the region where triply quantized vortices will be energetically stable. Therefore, formation of vortices with $L = 3$ from vortices with $L = 2$ would be possible either with the appearance of a singly-quantized vortex, that is not energetically advantageous in this region, or through a relatively unlikely 'many-particle process', where e.g. three doubly quantized vortices simultaneously transform into two vortices with $L = 3$. The

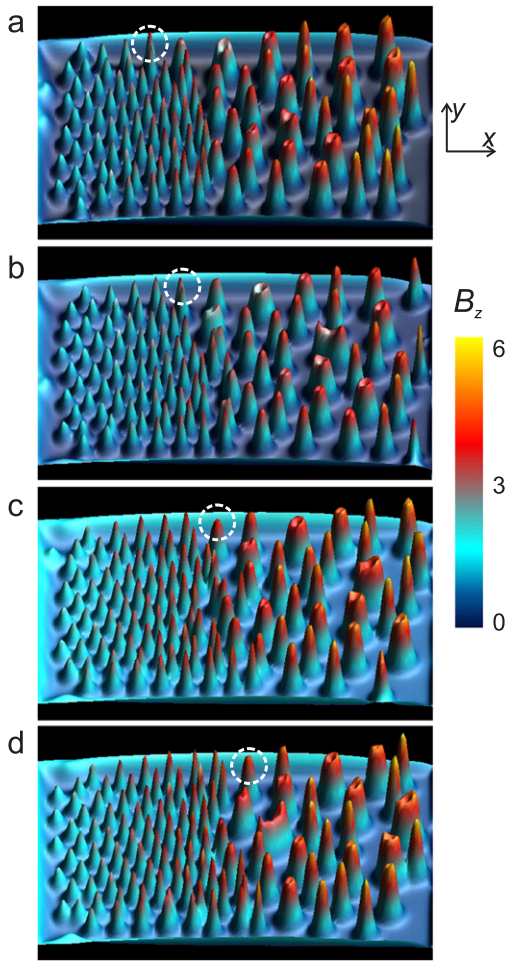

Figure 4. Four snapshots of the z component of the magnetic field in the superconductor, averaged over its thickness, for a wedge with $\xi = 250$ nm, $\lambda = 50$ nm, L_x=10 μm, L_y=15 μm, $d_{\min} = 20$ nm, and $d_{\max} = 200$ nm at $B_0 = 1$ and $j_e = 0.05$. Time increases from (a)–(d) with a constant step $\Delta t = 40$. The single-quantum vortices, which enter the sample through the lhs boundary, merge into giant vortices when propagating towards the rhs boundary (see, for example, the two single-quantum vortices marked with the dashed circle in panel (a) and their evolution in (b)–(d)).

obtained results together with the above arguments suggest an obvious generalization: in the regime under consideration the winding number, resulting from vortex coalescence, should preferentially (or even exclusively) take the values 2^n with $n = 1, 2, 3, \ldots$ Our simulations imply that, although at high current densities the vortex dynamics becomes less regular and the aforedescribed regime can be violated, the range of j_e where this regime persists is relatively wide (see supporting information).

4. Conclusions

The results of our TDGL simulations imply that a type-I superconductor wedge can provide a convenient playground to study a gradual transition between the effectively type-II and type-I superconducting behaviours. The simulated equilibrium vortex patterns demonstrate, in particular, the existence of stable singly quantized vortices even in the thickest part of the wedge—in a qualitative agreement with the experimental SHPM data for thick films of type-I superconductors. We have also analysed the vortex dynamics and the processes of vortex merging in the presence of an externally applied current, which causes vortex flow from the thinner part of the wedge to its thicker part. It is shown that these processes can result in a regime where only vortices with winding numbers equal to powers of two are present in the sample (except for its thickest edge, where the winding number of a giant vortex decreases with time step by step). While a direct experimental monitoring of the described vortex dynamics seems to be a rather challenging task, it should be possible to experimentally verify the predicted regime by studying (e.g., with SHPM) the corresponding static vortex patterns after switching off the external current.

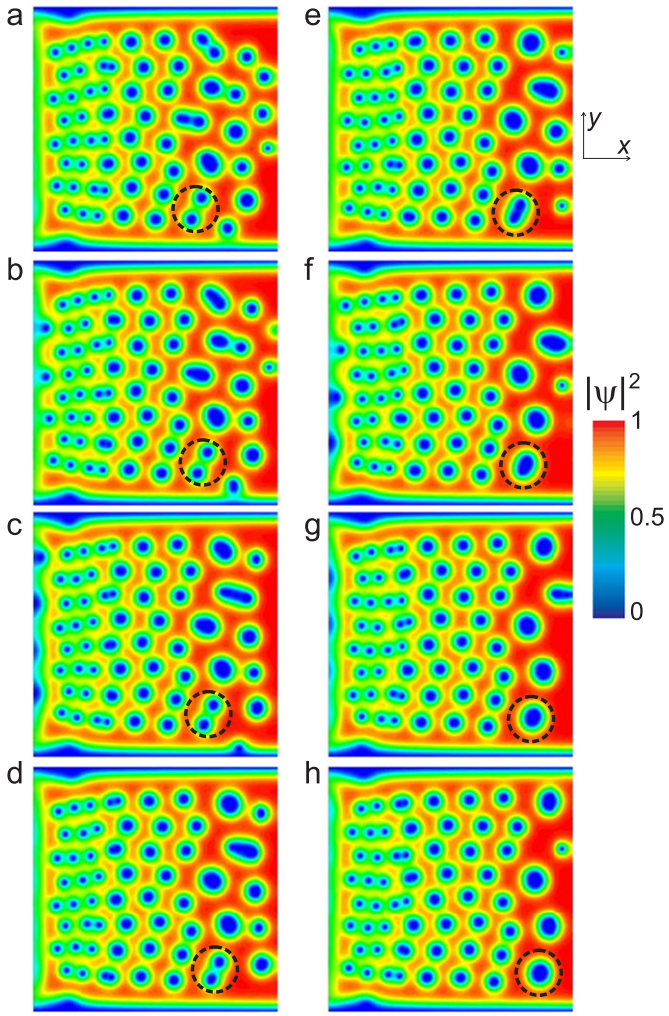

Figure 5. Eight snapshots of the calculated order parameter distribution for a wedge with $\xi = 250$ nm, $\lambda = 50$ nm, L_x=10 μm, L_y=10 μm, $d_{\min} = 20$ nm, and $d_{\max} = 200$ nm at $B_0 = 1$ and $j_e = 0.05$. Time increases from (a)–(h) with a constant step $\Delta t = 10$. Only vortices with $L = 2^n$ ($n = 1, 2$) are formed as a result of vortex coalescence. The dashed circle indicates two giant vortices with $L = 2$, which further merge into a giant vortex with $L = 4$.

Acknowledgments

This work was supported by Methusalem funding by the Flemish government and by the Fund for Scientific Research-Flanders, through FWO-V projects G.0115.12N, G.0119.12N, G.0429.15N, and the WOG WO.033.09N. The authors also gratefully acknowledge support of the Research Fund of the University of Antwerp.

References

[1] Abrikosov A A 1957 *Sov. Phys.—JETP* **5** 1174
[2] Jeudy V, Gourdon C and Okada T 2004 *Phys. Rev. Lett.* **92** 147001
[3] Berdiyorov G R, Hernandez A D and Peeters F M 2009 *Phys. Rev. Lett.* **103** 267002
[4] Ge J, Gutierrez J, Cuppens J and Moshchalkov V V 2013 *Phys. Rev.* B **88** 174503
[5] Tinkham M 1963 *Phys. Rev.* **129** 2413
[6] Parks R D and Mochel J M 1963 *Phys. Rev. Lett.* **11** 354
[7] Pearl J 1964 *Appl. Phys. Lett.* **5** 65
[8] Engbarth M A, Bending S J and Milosevic M V 2011 *Phys. Rev.* B **83** 224504
[9] de Gennes P G 1999 *Superconductivity of Metals and Alloys* (Oxford: Westview Press)
[10] Yampolskii S V and Peeters F M 2000 *Phys. Rev.* B **62** 9663
[11] van de Vondel J, Gladilin V N, Silhanek A V, Gillijns W, Tempere J, Devreese J T and Moshchalkov V V 2001 *Phys. Rev. Lett.* **106** 137003
[12] Chapman S J, Du Q and Gunzburger M D 1996 *Z. Angew. Math. Phys.* **47** 410
[13] Auer J and Ullmaier H 1973 *Phys. Rev.* B **7** 136
[14] Klein U 1987 *J. Low Temp. Phys.* **69** 1
[15] Ge J, Gutierrez J, Lyashchenko A, Filipov V, Li J and Moshchalkov V V 2014 *Phys. Rev.* B **90** 184511

[16] Tinkham M 1996 *Introduction to Superconductivity* 2nd edn (New York: McGraw-Hill)
[17] Kato R, Enomoto Y and Maekawa S 1991 *Phys. Rev.* B **44** 6916
[18] Silhanek A V, Gladilin V N, van de Vondel J, Raes B, Ataklti G W, Gillijns W, Tempere J, Devreese J T and Moshchalkov V V 2011 *Supercond. Sci. Technol.* **24** 024007
[19] Gladilin V N, Tempere J, Devreese J T and Moshchalkov V V 2012 *Solid State Commun.* **152** 1781
[20] Cerbu D, Gladilin V N, Cuppens J, Fritzsche J, Tempere J, Devreese J T, Moshchalkov V V, Silhanek A V and van de Vondel J 2013 *New J. Phys.* **15** 063022
[21] Pearl J 1966 *J. Appl. Phys.* **37** 4139
[22] Chang A M, Hallen H D, Harriott L, Hess H F, Kao H L, Kwo J, Miller R E, Wolfe R, van der Ziel J and Chang T Y 1992 *Appl. Phys. Lett.* **61** 1974
[23] Ge J, Gutierrez J, Gladilin V N, Devreese J T and Moshchalkov V V 2015 *Nat. Commun.* **6** 6573